Acta of Bioengineering and Biomechanics
Vol. 21, No. 1, 2019

Original paper
DOI: 10.5277/ABB-01268-2018-02

An exoskeleton arm optimal configuration determination using inverse kinematics and genetic algorithm

SEBASTIAN GŁOWIŃSKI, ANDRZEJ BLAŻEJEWSKI*

Koszalin University of Technology, Faculty of Technology and Education,
Department of Mechatronics and Applied Mechanics, Koszalin, Poland.

Purpose: This paper deals with the kinematic modelling of an arm exoskeleton used for human rehabilitation. The biomechanics of the arm was studied and the 9 Degrees of Freedom model was obtained. The particular (optimal) exoskeleton arm configuration is needed, depending on patient abilities and possibility or other users activity. *Methods:* The model of upper arm was obtained by using Denavit–Hartenberg notation. The exoskeleton human arm was modelled in MathWorks package. The multi-criteria optimization procedure was formulated to plan the motion of trajectory. In order to find the problem solution, an artificial intelligence method was used. *Results:* The optimal solutions were found applying a genetic algorithm. Two variants of motion with and the visualization of the change of joints angles were shown. By the use of genetic algorithms, movement trajectory with the Pareto-optimum solutions has been presented as well. Creating a utopia point, it was possible to select only one solution from Pareto-optimum results. *Conclusions:* The obtained results demonstrate the efficiency of the proposed approach that can be utilized to analyse the kinematics and dynamics of exoskeletons using the dedicated design process. Genetic algorithm solution could be implemented to command actuators, especially in the case of multi-criteria problems. Moreover, the effectiveness of this method should be evaluated in the future by real experiments.

Key words: *arm exoskeleton, genetic algorithm, inverse kinematics*

Symbols and notation

a_i – the i-link length [m]
d_i – the i-link offset [m]
α_i – the i-link twist [deg]
β – min and max human joint [deg]
q – the decision variable vector
q_i – the specification i-link
$[q_i]$ – the joint positions vector
q_α, q_β – the optimization problem solutions
q_{C1}, q_{C2} – the individuals who are the next generation
q_{p1}, q_{p2} – the generation of the parents
q_{si}, q_{fi} – the initial and final angle of the i-joint [deg]
θ_i – the i-joint angle [deg]
F_{obj} – the objective function
K_1, K_2, K_3 – the criteria of Pareto-optimal solution
S, S^* – the strings in which the numbers 0 and 1 are swapped
d_b – the distance between the base and the first coordinate set [m]
l_a – the length of an arm [m]
l_f – the length of a forearm [m]
l_w – the length of a wrist [m]
x_i, y_i, z_i – the coordinates of the i-joint
m_j – is mass of each arm M elements
x_s, y_s, z_s – the initial position of the effector
x_f, y_f, z_f – the final position of the effector

1. Introduction

Exoskeletons are a new class of articulated mechanical systems whose performance is accomplished while in intimate contact with a human user. Some of them are designed to be worn by the operator, having a similar kinematic structure to a human limb. The focus was on the application of active exoskeletons

* Corresponding author: Andrzej Blazejewski, Koszalin University of Technology, ul. Śniadeckich 2, 75-453 Koszalin, Poland. Phone: +48 602 327 002, e-mail: andrzej.blazejewski@tu.koszalin.pl

Received: December 7th, 2018
Accepted for publication: February 11th, 2019

for industry and medical purposes [12], [23]. In medical cases, exoskeletons can support motion therapy or support other kind therapies, especially osteoporosis, rheumatoid diseases and other diseases of cartilage occurring in human joints [24], [25]. The exoskeletons force proper patient movements, which is combined with magneto-therapy. For soldiers in the field (infantry) they can offer greater load carrying mobility with less strain and ability to walk further distances. For military aircraft services they could remove load from workers to avoid wearing down their bodies through strenuous physical work (e.g., suspending arms). In the emergency for firefighters, the most significant benefit is the ability to climb many flights of stairs with much more weight without fatigue. For patients, they can offer assistance during their rehabilitation process by guiding motions on correct trajectories to help to relearn motion patterns. Sometimes they give force support to be able to perform certain motions (which is necessary for the rehabilitation process) [7]. Moreover, they are able to treat the patient without the presence of the therapist, enabling more frequent treatment and potentially reducing costs.

Table 1. Minimum DoF for arm exoskeleton joints

Joints	DoF	Description
Spine segments	3	Flexion/extension, lateral flexion, rotation
Shoulder	3	Flexion/extension, abduction/adduction, rotation
Elbow	2	Flexion, forearm pronation/supination
Wrist	2	Flexion/extension, abduction/adduction

Many researchers have devoted to the study of an exoskeleton arm. Pons et al. [18] provided a comprehensive discussion of the field of exoskeletons, which are called wearable robots. They have taken biomechatronic design into account, cognitive and physical human-robot interaction, wearable robot technologies, kinematics, dynamics and control. Rocon et al. [19] focused on the area of rehabilitation robotics with medical problems and experiments using exoskeletons. The human arm kinematics and dynamics during daily activities were analysed in [22], whereas the design and preliminary evaluation of an exoskeleton for upper limb were presented in [10]. Determining the values of kinematic parameters describing human locomotion was successfully analysed and presented in [17]. The authors presented ranges of motion of joints, the instantaneous values of joint angles and change in dynamics of these values, which could be used for analysing human motion. Forward and inverse kinematics play a key role in determining property position of an exoskeleton arm. The biggest problem is the selection of a suitable method. Authors of the paper [16] proposed the generalization in solving mechanics (kinematics and dynamics) of manipulators with an application of a PC. They presented 4×4 homogenous transformation matrices and described problems of rotation and translation of manipulator links using MATLAB-Simulink package with Robotics Toolbox for simulation [5]. Some of the solutions and procedures have been presented in [1]. Asfour and Dillmann [2] proposed the use of redundancy for the generation of human-like robot arm motions with a suggestion of a variety of hypothetical cost functions to explain principles of the human arm movements. They successfully applied this method to the generation of human-like motions of the humanoid robot ARMAR. Another approach to planning the trajectory of an exoskeleton was proposed [11]. In this paper, we consider the problem of generating exoskeleton-human-like motions from the kinematics' point of view. We propose to consider a 9 Degree of Freedom (DoF) model of an exoskeleton arm as a basis and the use of a genetic algorithm method to calculate a proper position applying inverse kinematic of exoskeleton arm.

2. Materials and methods

2.1. Human arm (kinematics)

The investigated structure of the upper limb has been divided into three segments: the arm, the forearm and the hand [8]. An arm is a region between a shoulder and an elbow. A torso and an arm are connected by a shoulder, an arm and a forearm by elbow, whereas a forearm and a hand by a wrist. According to the study by the Army Research Laboratory, detailed requirements for an arm exoskeleton suggests a minimum number of DoF [6].

The movements of the shoulder are shown in Fig. 1a. Circumduction is a circular movement that combines flexion/extension, abduction/adduction [15], [17]. The elbow with 2DoF links the upper and lower arm, and the movement is presented in Fig. 1b. The wrist-linking forearm and hand (end-effector) may be considered as having 2 DoF: abduction/adduction and flexion/extension (Fig. 1c).

Figure 2 shows the 10 DoF exoskeleton model, where Z_i represent axis of the degree of freedom in i direction. The five joints include 10 DoF (base and

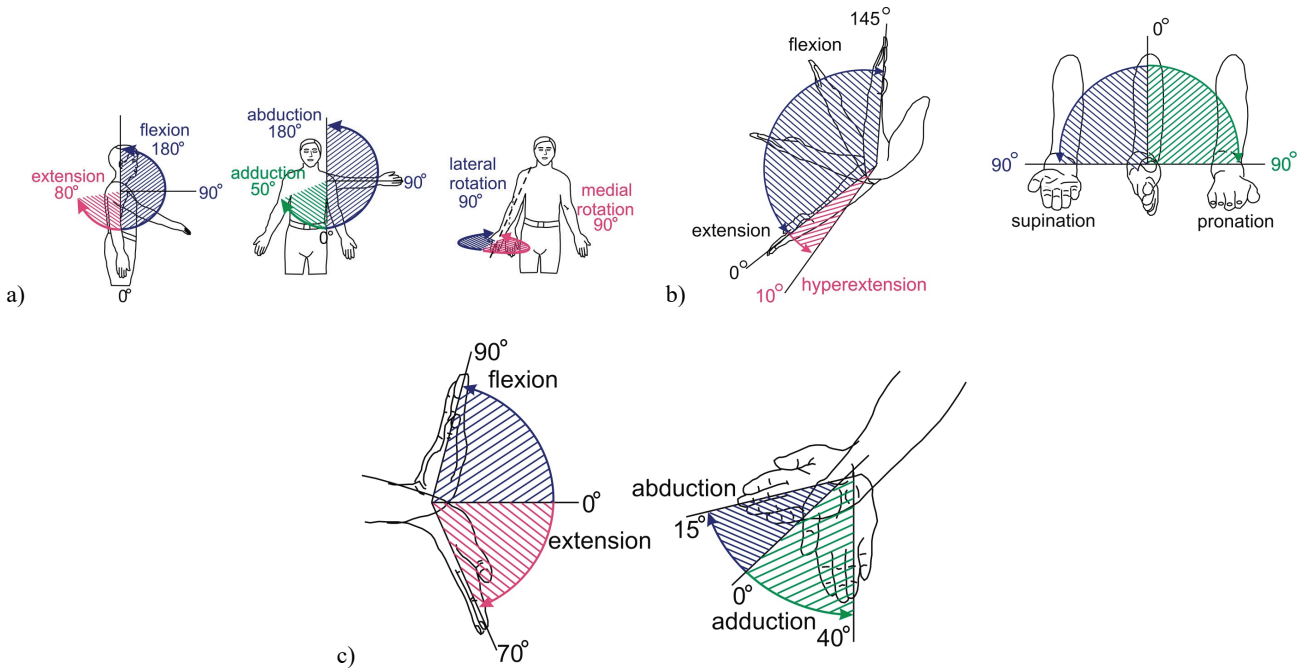

Fig. 1. Human joint movement: a) shoulder, b) elbow c) wrist

spine joint – 2 DoF, shoulder joint – 3 DoF, elbow joint – 2 DoF and, wrist joint 2 DoF) creating a redundant 10 DoF model of the exoskeleton arm. The exoskeleton structure is adjustable to accommodate a wide range of operator sizes. It should be able to accommodate from the 5% of female to the 95% of male size [13]. The body segment lengths a_i and d_i are constant for each individual and it is necessary to estimate these parameters (Fig. 2). Body segment characteristics are the dimensions of the arm parts, its mass, center of mass and their moments of inertia. These lengths scale with the total height of the person and can be approximated as [11].

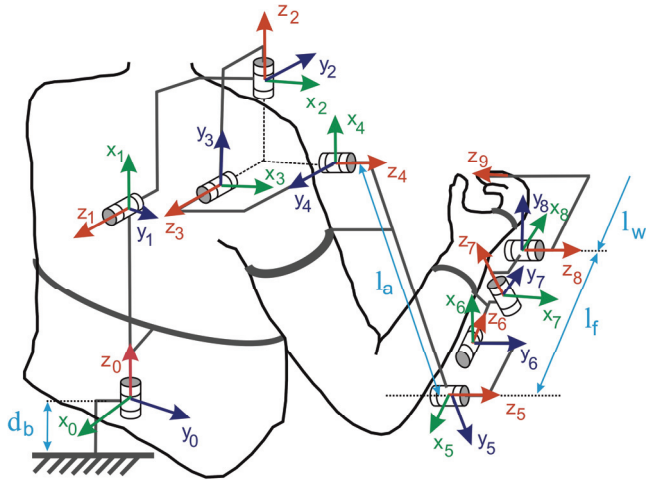

Fig. 2. Coordinate systems of the exoskeleton and degree of freedom axes Z_i

To control the end-effector, it is necessary to determine the relationship between joints and the position and orientation links.

2.2. Denavit–Hartenberg convention

For selecting reference frames in exoskeleton applications, the D–H convention is very often applied [9], [14], [21]. The values of the kinematic parameters of the 9DoF (without finger (Z_9)) exoskeleton arm by using the D-H convention are listed in Table 2. The inverse problem function is formulated in the following, general form:

$$[q_i] = F([x_f, y_f, z_f], q_i^S) \tag{1}$$

It means, that it is possible to obtain a set of general displacement of the joints, when the initial position of each i joint is represented by q_i^S and target point coordinates [x_f, y_f, z_f] (final position of the end--efector) are known. According to D–H convention and introducing (1), (2), (3) and (4), the [q_i] implicate [x_i, y_i, z_i] finally.

In Table 2, parameters β are limitation of joints movement (Fig. 1), Num – number of links; finger (Z_9) is not considered in this work further, parameters d_b, l_a, l_f and l_w are shown in Fig. 2.

Table 2. D-H parameters for exoskeleton segments – constraints

Joint	β	Num	α_i	a_i	d_i	θ_i
Base (z_0)	±45°	1(0 → 1)	90°	0	d_{base}	q_1
Spine (z_1)	±15°	2(1 → 2)	–90°	a_2	d_2	q_2
Shoulder (z_2)	±90° med/lat rotation	3(2 → 3)	90°	0	0	q_3
Shoulder (z_3)	–180° abd/add +50°	4(3 → 4)	90°	0	0	q_4
Shoulder (z_4)	–180° flex/ext +80°	5(4 → 5)	0°	l_{arm}	0	q_5
Elbow (z_5)	–10° ext/flex +145°	6(5 → 6)	90°	0	0	q_6
Spine (z_6)	±90° pron/sup	7(6 → 7)	–90°	0	l_{forearm}	q_7
Wrist (z_7)	–90° flex/ext +70°	8(7 → 8)	–90°	0	0	q_8
Wrist (z_8)	–15° abd/add +40°	9(8 → 9)	0°	l_{wrist}	0	q_9

2.3. Formulation an optimization problem, objective function and decision variables

The multi-objective function F_{obj} is created (2), using inverse kinematics and function (1). The decision variables are sets of general displacements of each joint $[q_i]$. The main problem is to find the solution minimizing simultaneously three criteria (3). First criterion K_1 (4) is the distance between end-effector and the set target point in 3D Cartesian space. Second criterion K_2 (5) is the sum of total change angles in all joints when the arm changes the position. Third criterion K_3 (6) indicates differences between potential energy of arm in a particular position and the arm potential energy in an initial position.

The sought solution should be closest to the indicated target point and should assure minimal change of angles in joints and potential energy of the exoskeleton. The optimization problem can be presented in the following form:

– objective function F_{obj} and decision variables $[q_i]$:

$$K_1, K_2, K_3 = F_{\text{obj}}([q_i]); \tag{2}$$

– optimization problem and sought (Pareto-optimal) solutions $[q_i^O]$:

$$\min_{q_{\min} \le q_i \le q_{\max}} [K_1 \wedge K_2 \wedge K_3] \rightarrow [q_i^O]; \tag{3}$$

– criteria K_1, K_2, K_3:

$$K_1 = \sqrt{(x_{\text{end}} - x_f)^2 + (y_{\text{end}} - y_f)^2 + (z_{\text{end}} - z_f)^2}\ , \tag{4}$$

$$K_2 = \sum_{i=1}^{N} | q_i^S - q_i^{\text{end}} |, \tag{5}$$

$$K_3 = \sum_{j=1}^{M} m_j g z_j^m - E_p^0, \tag{6}$$

where x_{end}, y_{end}, z_{end} are coordinates of the effector final points in Cartesian space (position of the end-effector) and x_f, y_f, z_f, represent the target point coordinates, q_i^S is the initial angle of the i-joint and q_i^{end} represents final angle of the i-joint (1) (total joints angel change). The initial angle of i-joint $[q_i^S] = [q_1 = 0, q_2 = 0, q_3 = 0, q_4 = -\pi/2, q_5 = 0, q_6 = \pi/2, q_7 = \pi/2, q_8 = -\pi/2, q_9 = 0]$ results $[x_s, y_s, z_s]$. The paremeters $q_{\min}$ and $q_{\max}$ represent the bounds, the limits of q_i variation (Fig. 1), m_j is mass of each arm M elements, z_j^m represents a z-coordinate difference in relation to arm initial position, where its potential energy is E_p^0 and, finally, g is an acceleration of gravity. The Pareto-optimal solutions $[q_i^O]$, within feasible solutions, can be obtained in the form surface, in the case of three criteria.

2.4. Pareto-optimal solutions indication method

In order to obtain solutions $[q_i^O]$, i.e., the decision variables values, which result in the objective function F_{obj} (2), return for values of criteria K_1, K_2, K_3 (3), the GA method is proposed. It is based on iterative selection, crossover and mutation processes in order to find the Pareto-optimal solutions. These solutions must meet the criterion of Pareto-optimality i.e., must be nondominated [3], [4]. The number of solutions considered in each iteration is called population, and the particular solution is called an individual (or chromosome). Each individual consists of particular configuration of design variables called genes. The number of

individuals introduced as arguments of an objective function is called generation. During each iteration among the chosen population, which is obtained by calculating objective function F_{obj} (2) implementing selected decision variables $[q_i]$, the process of non-dominated solutions is conducted. The selection is done introducing a ranking process. Each solution $[q_i]$, depending on whether the solution is dominated or not, is assigned to a particular rank. In the next step, the roulette method is used to designate the parents i.e., specific solutions $[q_i^P]$ which are involved in new population creation, by their children $[q_i^C]$.

In this way, pairs of the parents ($[q_i^{P1}]$ and $[q_i^{P2}]$) are created and the roulette procedure is repeated until a number of turns reaches a half of the population size. In the next step, the selected pair of parents forms a new generation including their children $[q_i^C]$, which are created using crossover and mutation mechanism. The last step is a mutation where the decision variables are randomly changed just like position of the vector of decision variables. The selection process in one iteration is over in this way. After the last of the iteration, Pareto-optimal solutions are returned. The introduced GA procedure, which allows to search and indicate nondominated solutions, is totally implemented in Matlab function developed by Popov and added and available as Matlab toolbox.

3. Results

The decision variables appearing in the formulation of the objective function (2) and its minimization (3) are the discrete value of angles in the exoskeleton joints. In this particular arm problem consideration, the finger Z_9 DOF (Fig. 2) is omitted. In this case, nine joint positions are indicated ($N = 9$):

$$[q_i] = [q_1, q_2, q_3, q_4, q_5, q_6, q_7, q_8, q_9] \tag{7}$$

It means that one individual contains nine genes. The numbers of joins are related to coordinate systems of the exoskeleton shown in Fig. 2. The $q_i = 1$ is related to z_0 and, subsequently with z axes numbering $q_i = 9$, is related to z_8 joint.

Furthermore, the constraints $q_{\min}$ and $q_{\max}$ of positioning accuracy are imposed on decision variables according to Table 2 and, particularly, parameter β. To obtain the minimal value of the objsective function with three criteria (4), (5) and (6), the GA is used, with initial population of 50 (constant value during the whole process) and 6×104 iterations. It is done by searching the solutions applying requirements. Considered are only the solutions where the distance between end-effector and the target point (4) is less than 5 mm. It is the constraint imposed on criterion K_1 in order to establish the accuracy of the exoskeleton arm. Additionally, trajectory under the assumption that each joint is changed during the arm movement with constant angular velocity is estimated.

3.1. The Pareto-optimal solution in case of the 9 Dof exoskeleton arm

There are chosen example cases of target point $[x_f, y_f, z_f]$, and the same q_i^S initial the arm position (1). The initial configuration q_i^S, which subsequently allows for calculating x_{end}, y_{end}, z_{end}, i.e., coordinates of the initial end-effector position, introduced in (4). The 25 is a limit of Pareto-optimal solutions, which are presented in the figures in the form of Pareto surface.

The Pareto-optimum solutions distribution depicted in criteria coordinates (blue points) are presented in Figs. 3–4 a). By creating a utopia points (marked as red circles), only one particular solution is chosen, as the best solution from the Pareto-optimum solutions, which is the nearest to the point of utopia. In the adjacent figures, arm configurations and trajectory related to chosen Pareto-optimal solutions are shown. In Figs. 3 and 4 b–d, mark B displays the target point in 3D Cartesian space. The trajectory (solid line —) connecting the initial position mark as A to final position B. The two target points and initial arm configurations cases are investigated. There are two initial arms configuration: arm bent at the elbow (case 1) and arm position straight down (case 2). The arm with joints is depicted as a dashed line with circles (−∘−). The arm positions, starting from initial, through intermediate, to final one are marked using progressively bolder dashed lines. Initial end-effector position $[x_{\text{end}}, y_{\text{end}}, z_{\text{end}}]$ = [230.220, 700.002, −110.32] [mm] is constant in following investigated case.

3.2. Case 1

Results in the case of first situation, where target point position one $[x_f, y_f, z_f]$ = [230.220, 1010.322, 200.0] [mm] are presented. The solutions $[q_i^O]$ obtained $[q_i^O]$ in the case of criteria minimal values K_1 = 0.6168 mm, K_2 = 228.2435 deg and K_3 =

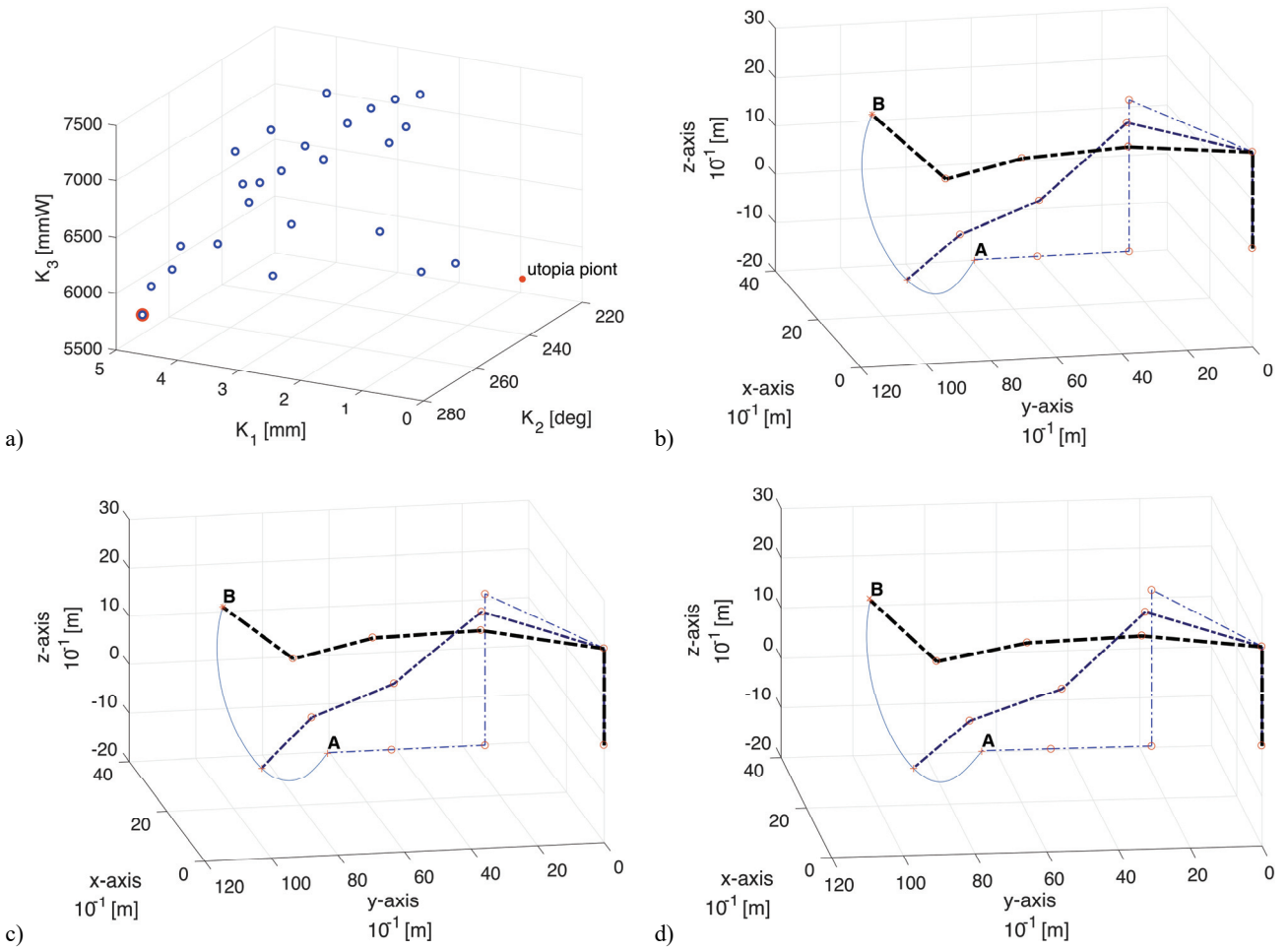

Fig. 3. End-effector target point – case 1, a) Pareto-optimal solutions and arm configuration in the case of criterion: b) K_1 minimal value, c) K_2 minimal value, d) K_3 minimal value and simultaneously solution nearest utopia point

5773.8 mW get the following values using deg units, respectively:

$$[q_i^O]^{K_1} = [16.515, -13.548, 17.360, 1.539,$$

$$-51.730, 74.076, -19.997, -41.837, 24.752];$$

$$[q_i^O]^{K_2} = [16.515, -7.739, 17.450, -0.047,$$

$$-51.730, 73.076, 0.018, -40.535, 21.135];$$

$$[q_i^O]^{K_3} = [16.737, -14.968, 17.487, -0.373,$$

$$-51.803, 75.901, -21.171, -45.543, 32.189].$$

Figures 3b–d show arm's parts configuration, related to above solutions, respectively.

3.3. Case 2

Results in the case of the second situation, where target point position $[x_f, y_f, z_f]$ = [460.400, 500.0, 400.0] [mm] are presented. The solutions $[q_i^O]$ obtained $[q_i^O]$ in the case of criteria minimal values K_1 = 3.9117 mm, K_2 = 304.6875 deg and K_3 = 7809.4 mW, get the following values using deg units, respectively:

$$[q_i^O]^{K_1} = [25.058, -0.141, -33.658, 45.779,$$

$$-81.742, 75.796, -0.027, -88.134, -0.014];$$

$$[q_i^O]^{K_2} = [25.058, 0.047, -33.678, 0.304,$$

$$-81.742, 75.686, -0.027, -88.134, -0.014];$$

$$[q_i^O]^{K_3} = [24.943, -0.311, -33.678, -89.963,$$

$$-81.698, 76.006, 80.922, -89.393, 0.965].$$

Figures 4b–d show arm's parts configuration, related to the above solutions, respectively.

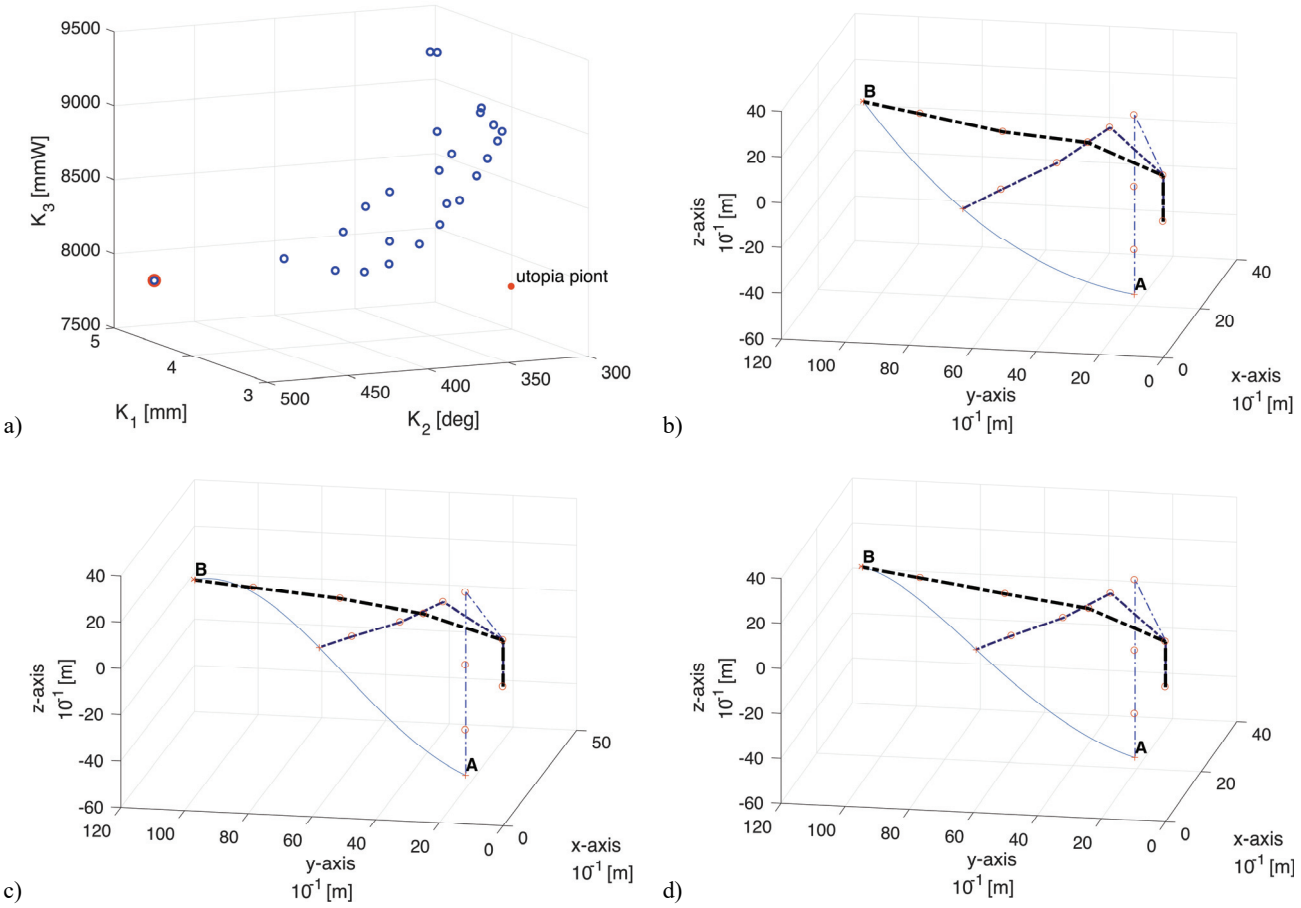

Fig. 4. End-effector target point – case 2, a) Pareto-optimal solutions and arm configuration in the case of criterion: b) K_1 minimal value, c) K_2 minimal value, d) K_3 minimal value and simultaneously solution nearest utopia point

4. Discussion

This work had several goals. The main one was to create the 9DoF model of exoskeleton arm by using D–H notation. At first, the angles and torques have been estimated from biomechanical data collected from humans. The maximal workspace of exoskeleton arm was successfully determined with the variability of the joint limits and limb, which is dependent on a person's height.

In previous works which dealt with this kind of problem, the inverse kinetic and DH notation were applied successfully, as presented in papers [10], [11] and in other works as well. The required position of end-effector was worked out using gradient methods. These algorithms are very effective in the smooth objective functions case. When objective function based on DH notation is created considering the limited number of criteria (one or two like in the papers [10], [11]), the smoothness is achieved very often and the gradient methods should work, it gives one particular solution. But, in the case when the objective function becomes multi-criterial, there could be more than one solution or solutions laying down very close to each other. In that case gradient method fails. Which solution is required and finally should be considered, contrary to other? The gradient algorithm does not find it, because it pointed out just one solution. It may be determined considering some set of solutions (Pareto-solution) in the criteria domain (n-dimensional domain, where n is the number of criteria).

Therefore, as an alternative for that approach, the following strategy was proposed: to combine GA method with solutions obtained using the inverse kinematics of exoskeleton arm. It is foreseen to be useful at least for engineers in robotics and in the rehabilitation process. For example, this GA solution could be implemented to command and control actuators in a robotic state or to lead arm in the case of it being disabled. Three necessary criteria were provided to determine whether correct solutions existed

without using forward kinematics. By using GA, moving trajectory with the Pareto-optimum solutions has been presented. By creating a utopia point it was possible to select only one solution from Pareto-optimum results by choosing a solution that was closest to the utopia point. The operating time of the GA does not enable us to use it in real time application, but to determine the optimum solution in terms of the selected criteria. The further work needs to be done. We have only focused on the problem associated with inverse kinematics, whereas trajectory energy optimization (next criteria) should be analysed. The presented approach does not consider the dynamics of the exoskeleton arm. The operating time of the GA to obtain Pareto-optimum solutions in the examples presented above is approximately 30–31 minutes per task. It does not allow to use this procedure in real-time application, but it can be used to determine the optimum solution in terms of the selected criterion.

5. Conclusion

The obtained solution can be collected before the physical exoskeleton movement procedure. By creating the data based on the possible destinations for the end-effector it will be possible to choose the right solution and use it in real time. It is also shown that this approach allows to plan or design the trajectory. Knowing initial or neutral arm position and determining optimal arm configuration at the final position, it is possible, on the one hand, to assign the trajectory under particular joints velocity profile, and, on the other hand, to create the velocity profile for each joint, so as to get a desirable trajectory. The so-called optimal positions and trajectory, in the case of this kind of problem, have to be chosen from the multi-solution set. The new approach, presented in this work, was not introduced so far for this specific purpose, but basing on genetic algorithm (artificial intelligence) application gives a relatively fast and desirable accurate result. It will be investigated in future work. Moreover, the effectiveness of this method should be evaluated in the future by real experiments. The next step will be to find out the dynamics' parameters, such as moment inertia and torques. Calculated torques in each arm joint allow select actuators for exoskeleton.

References

[1] ALRASHIDI M., YILDIZ I., VANAT Q., ESAT M., CHIZARI M., *Kinematics Analysis of the Elbow Joint; Comparison of the Kinematics of the Left and Right Elbow*, Proceedings of the World Congress on Engineering, Jul. 6–8, 2011, 2681–2684.

[2] ASFOUR T., DILLMANN R., *Human-like Motion of a Humanoid Robot Arm Based on a Closed-Form Solution of the Inverse Kinematics Problem*, IEEE/RSJ Intern. Conf. on Intelligent Robots and Systems, USA, 2003, 1407–1412.

[3] BLAZEJEWSKI A., *Reduction of low frequency acoustical resonances inside bounded space using eigenvalue problem solutions and topology optimization*, Theoretical and Experimental Analysis. Springer Proceedings in Mathematics and Statistics, 2016, 182, 15–25.

[4] BLAZEJEWSKI A., *Topology optimization of a bounded space for a vibroacoustical problem in a low frequency*, Solid State Phenomena, 2016, 248, 41–48.

[5] CORKE P., *Robotics*, Vision and Control, Fundamental Algorithms in MATLAB, Springer, 2011.

[6] CROWELL H.P., *Human Engineering Design Guidelines for a Powered, Full Body Exoskeleton*, U.S. Army Research Laboratory, 1995.

[7] CULMER P., JACKSON A., LEVESLEY M., SAVAGE J., RICHARDSON R., COZENS J., BHAKTA B., *An admittance control scheme for a robotic upper-limb stroke rehabilitation system*, Engineering in Medicine and Biology 27th Annual Conference, 2005, 5081–5084.

[8] DAVIES D.V., DAVIES F., *Gray's Anatomy*, Green and Co., Ltd., 33 ed., 1962.

[9] DIJKSTRA E.J., *Upper Limb Project – Modeling of the Upper Limb*, Department of Engineering Technology, University of Twente, 2010.

[10] GLOWINSKI S., KRZYZYNSKI T., PECOLT S., MACIEJEWSKI I., *Design of motion trajectory of an arm exoskeleton*, Archive of Applied Mechanics, 2015, 85(1), 75–87.

[11] GLOWINSKI S., KRZYZYNSKI T., *An inverse kinematic algorithm for the human leg*, Journal of Theoretical and Applied Mechanics, 2016, 54(1), 53–61.

[12] GOEHLER C.M., *Design of A Humanoid Shoulder-Elbow Complex*, Dissertation, Aerospace And Mechanical Engineering Notre Dame, Indiana, 2007.

[13] JANSEN J., RICHARDSON B., PIN F., LIND R., BIRDWELL J., *Exoskeleton for Soldier Enhancement Systems Feasibility Study*, Oak Ridge National Laboratory, Tennessee, 2000.

[14] JAZAR R.N., *Theory of Applied Robotics*, Springer, 2007.

[15] LUTTGENS K., WELLS K.F., *Kinesiology: Scientific Basis of Human Motion*, 6th ed. Philadelphia: Saunders College Publishing, 1982.

[16] MILICEVIC I., SLAVKOVIC R., GOLUBOVIC D., *Industrial Robot Models Designing and Analysis with Application of Matlab Software*, Machine Design, 2007.

[17] PIETRASZEWSKI B., WINIARSKI S., JAROSZCZUK S., *Three-Dimensional Human Gait Pattern-Reference Data for normal Men*, Acta of Bioengineering and Biomechanics, 2012, 14(3), 9–16.

[18] PONS J.L., *Wearable Robots: Biomechatronic Exoskeletons*, John Wiley and Sons, 2008.

[19] ROCON E., PONS J.L., *Exoskeletons in Rehabilitation Robotics, Tremor Suppression*, Springer, 2011.

[21] SPONG M.W., HUTCHINSON S., VIDYASAGAR M., *Robot modeling and control*, Wiley, 2006.

[22] STASZKIEWICZ R., CHWAŁA W., FORCZEK W., LASKA J., *Influence of surface on Kinematic Gait Parameters and Lower Extremity Joints Mobility*, Acta of Bioengineering and Biomechanics, 2012, 14(1), 75–82.

[23] TZONG-MING W., DAR-ZEN C., *Design of an Exoskeleton for Strengthening the Upper Limb Muscle for Overextension Injury Prevention*, Mechanism and Machine Theory, 2011, 46, 1825–1839.

[24] WIERZCHOLSKI K., MISZCZAK A., *Magneto-therapy of human joint cartilage*, Acta of Bioengineering and Biomechanics, 2017, 19(1), 115–124.

[25] WIERZCHOLSKI K., *Time dependent human hip joint lubrication for periodic motion with stochastic asymmetric density function*, Acta of Bioengineering and Biomechanics, 2014, 16(1), 83–97.